Injection of CO_2 into an Unconfined Aquifer Located Beneath the Colorado Plateau, Central Utah.

S.P. White[1], R.G. Allis[2], J. Moore[3] T.Chidsey[2], C.Morgan[2], W. Gwynn[2], M.Adams[3]

[1]*Industrial Research Ltd, PO Box 31-310, Lower Hutt, New Zealand*
[2]*Utah Geological Survey, PO Box 146100, Salt Lake City, UT 84114, USA*
[3]*University of Utah, Salt Lake City, UT 84108, USA*

Abstract

This paper investigates injection of CO_2 into non-dome-shaped geological structures that do not provide the traps traditionally deemed necessary for the development of artificial CO_2 reservoirs.

We have developed a regional scale, two-dimensional numerical model of one such structure on the Colorado Plateau. This model includes the major physical and chemical processes induced by injection of CO_2 for 30 years at a rate of 5 million tonnes/year (equivalent to a 600 MW coal-fired power plant).

Ignoring water-rock reactions, CO_2 returns to the surface after about 250 years and about 40% remains sequestered after 1000 years. However, coupling water-rock reactions to transport calculations shows significantly more CO_2 is sequestered, with dawsonite and calcite the predominant sequestration minerals. There is still some leakage of CO_2 to the surface in all scenarios investigated but we estimate at least 70% remains permanently sequestered.

Introduction

This paper summarizes work investigating the injection of CO_2 into geological structures that are not dome shaped and thus do not provide the conventional reservoir-trap geology usually considered necessary for the development of a gas reservoir. Although such structures are open, they may however, provide very long flow paths between the injection point and the surface, allowing the permanent sequestration of the injected CO_2 as a mineral or dissolved in the groundwater. This type of structure is common in the Colorado Plateau and Southern Rocky Mountains region (Allis et al., these proceedings). A fuller description of the work is provided in White *et al.* (2003).

We investigate one such geological structure using a two-dimensional numerical model of an unconfined reservoir to study the long-term behavior of CO_2 injected in the reservoir. Using the reactive chemical transport code ChemTOUGH2 (White 1995) the model is able to represent the major physical and chemical processes induced by injection of CO_2 into the reservoirs including transport in the liquid and gas phases, the effect of dissolved CO_2 on brine density, and the reaction between the CO_2 plume and the reservoir rocks.

Geological Setting

The geology beneath Hunter Power Plant, located on the San Rafael Swell, is an example of a structure that, although not dome shaped, may provide a suitable CO_2 sequestration site. The San Rafael Swell is a major physiographic feature in east-central Utah. It represents a broad, basement-involved, asymmetrical anticline that trends north-northeast to south-southwest. The San Rafael Swell is one of numerous Laramide-age (middle to late Paleocene to early Oligocene) structures on the Colorado Plateau.

The site is considered an important test case as there are two power plants within 15 km with a combined capacity of 2000 MW producing 15 million tones of CO_2 emissions per annum. The sedimentary sequence shown in Figure 1 contains potential reservoir and seal formations at over 1 km depth beneath the power plant, but the regional dip exposes some of these formations at the surface some 40 to 50 km away.

Allis *et al*. (these proceedings) have reviewed he properties of likely reservoirs and capping structures in this region. Table 1 summarizes the properties of the units in the sequence and identifies several potential targets for the injection of CO_2 gas on this cross-section; 1) Navajo Sandstone, 2) Wingate Sandstone, 3) White Rim Sandstone, and 4) Redwall Limestone. Of these, only the Redwall Limestone is not exposed on the crest or flanks of the uplift.

Hydrological model

The regional topography and precipitation pattern give a pressure gradient roughly along the cross-section of Figure 1, with pressures highest in the West. Regional flow is from the high ground of the Wasach Plateau in the West towards the Green River in the East.

In the Wasach Plateau region (topography above about 2000 masl) annual precipitation ranges from 100 cm at the West of the section to 20 cm where the surface drops below 2000 masl. East of this the annual precipitation is 20 cm. Infiltration is taken to be 15% on the High Plateau, above 2500 masl and 2% elsewhere. These values are similar to those assumed by USGS hydrologic modeling of the Colorado Plateau, and one particular study of recharge amounts not too far from the cross-section of Figure 1 (Danielson and Hood, 1984).

Previous modeling studies simulated the formation of the natural CO_2 reservoirs at Farnham Dome on the Colorado Plateau (Allis *et al.* 2001, White *et al.* 2001, White *et al.* 2002). This work found that permeabilities of 100 mD for aquifers, 1 mD for mixed units, and 0.01 mD for confining units lead to the formation of the observed natural CO_2 reservoirs. Increasing these figures by an order of magnitude did not give rise to the formation of reservoirs.

On the eastern boundary of the model we set boundary pressures to those of a hydrostatic column with the water table depth determined from pressure measurements in the area while on the western boundary pressures are either hydrostatic or no flow across the boundary is enforced.

Formation	Typical Thickness (meters)	Age	Porosity	Permeability	Potential as a CO_2 Reservoir	Potential as a Seal
North Horn Tkn	<250	Tertiary	High	Med	Too shallow	
Price River Kpr	80	Cretaecous	High	Med	Too shallow	
Castlegate Kc	70	Cretaceous	High	High	Too shallow	
Blackhawk Kbh	120	Cretaceous	Med	High	Too shallow	
Star Point Ksp	60	Cretaceous	Med	Med	Too shallow	
Mancos Kmm	380	Cretaceous	Low	Low	Low	Med
Mancos Kmem	120	Cretaceous	Med	Med	Low	Med
Mancos Kmbg	200	Cretaceous	Low	Low	Low	High
Mancos Kmf	10	Cretaceous	High	High	Low	High
Mancos Kmt	20	Cretaceous	Low	Low	Low	High
Dakota and Cedar Mtn. Undivided Kdc	87	Cretaceous-Jurassic	Med	Med	Med	Low
Morrison Jms	201	Jurassic	Med	Med	Med	Low
Summerville/Curtis Js	82	Jurassic	Low	Low	Low	High
Entrada Je	136	Jurassic	Med	Low	Low	Low
Carmel Jc	82	Jurassic	Low	Low	Low	Med
Navajo Jn	160	Jurassic	High	High	High	Low
Kayenta Jk	53	Jurassic	Med	Med	Low	Low
Wingate Jw	107	Jurassic	High	High	High	Low
Chinle Trc	113	Triassic	Low	Low	Low	High
Moenkopi Trm	235	Triassic	Low	Low	Low	High
Black Box Pk	31	Permian	Med	Low	Low	Med
White Rim Pwr	153	Permian	High	High	High	Low
Elephant Canyon Pec	198	Permian	Low	Low	Low	Med
Honaker Trail Pht	190	Pennsylvanian	Med	Low	Low	Low
Paradox Pp	198	Pennsylvanian	Med	Low	Low	High
Pinkerton Trail Ppt	91	Pennsylvanian	Low	Low	Low	Med
Redwall Mr	244	Mississippian	Med	Med	Med	Low
Ouray Do	53	Devonian	Low	Low	Low	Med
Elbert De	76	Devonian	Low	Low	Low	Med
Lynch-Maxfield undivided Clm	312	Cambrian	Low	Low	Low	Med
Ophir Co	61	Cambrian	Low	Low	Low	High
Tintic Ct	62	Cambrian	Low	Low	Low	Low
Schist/Granite Pc	--	Precambrian	Low	Low	Low	Low

Table 1: Properties of geologic units forming the cross-section in Figure 1.

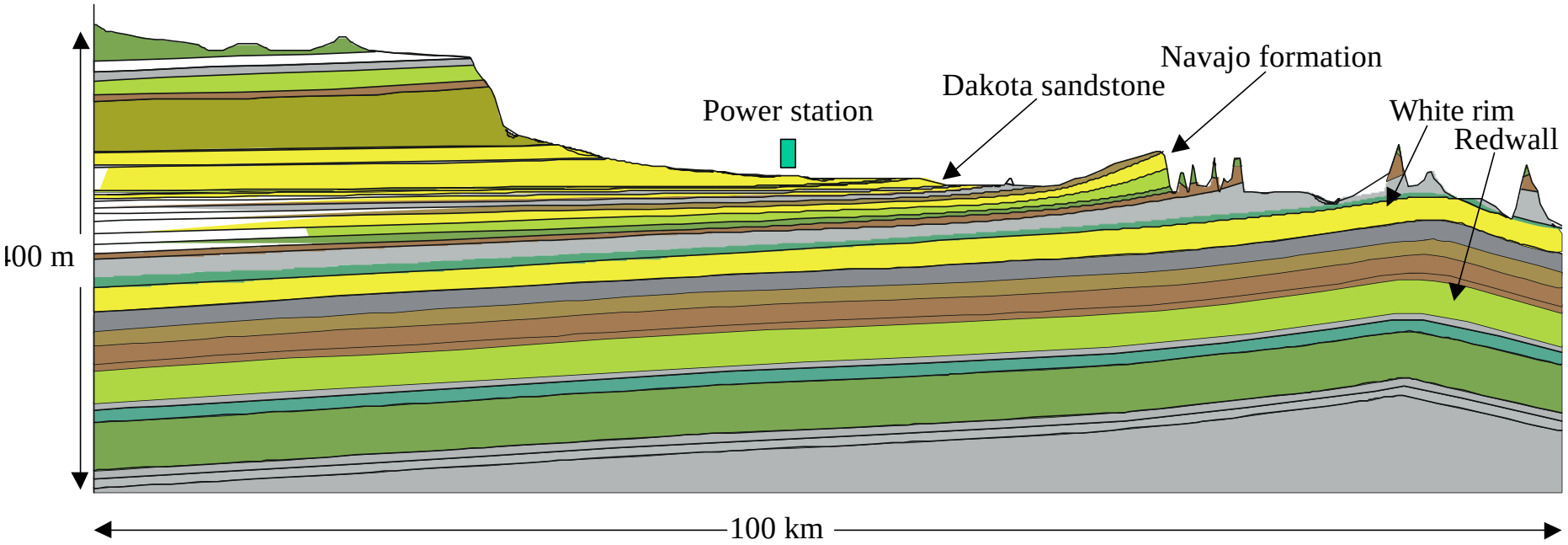

Figure 1: Geology on the cross-section beneath the Hunter Power-plant, Central Utah

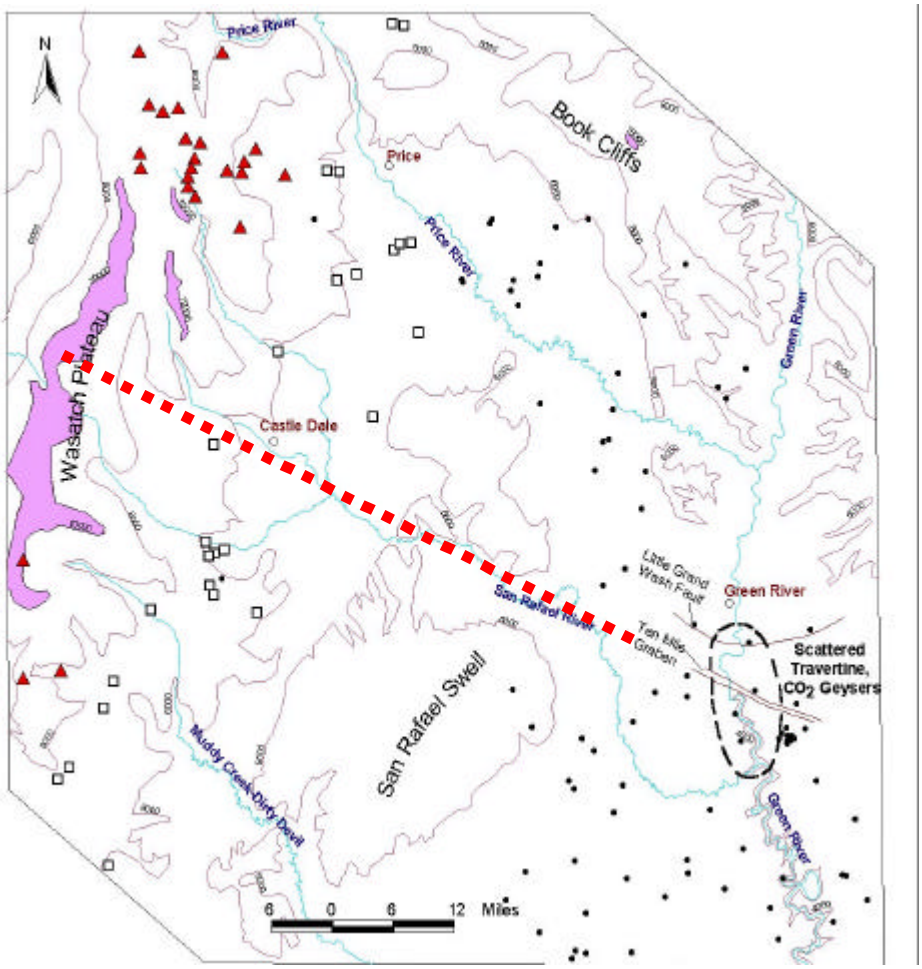

Figure 2: Cross-section on which the model is based. Symbols indicate the location of pressure data points used in calibrating the model. Data points on the East San Rafael Swell are to the east of the cross-section and provide a boundary condition on the Eastern boundary of the slice. Filled triangles on the Wasatch Plateau are the locations of downhole pressure data that provide a constraint on the west side of the cross-section. The lateral pressure gradient is about 10 MPa (100 bar).

Numerical Model

Two TOUGH2/ChemTOUGH2 integrated finite difference models of the cross-section shown in Figure 1 have been developed. In both models the cross-section is divided into a number of elements with element geometry determined by the need to match geological layer interfaces (Figure 3). In the first model (Model A) we have used a fine grid in the vicinity of the injection wells to resolve better the early part of the injection period when pressure gradients are large. Resolution in the second model (Model B) is reduced in order to keep the computer time requirements for modeling the CO_2-brine-rock interactions manageable. These models and the parameters used in the modeling are discussed in detail in White *et al*. (2003).

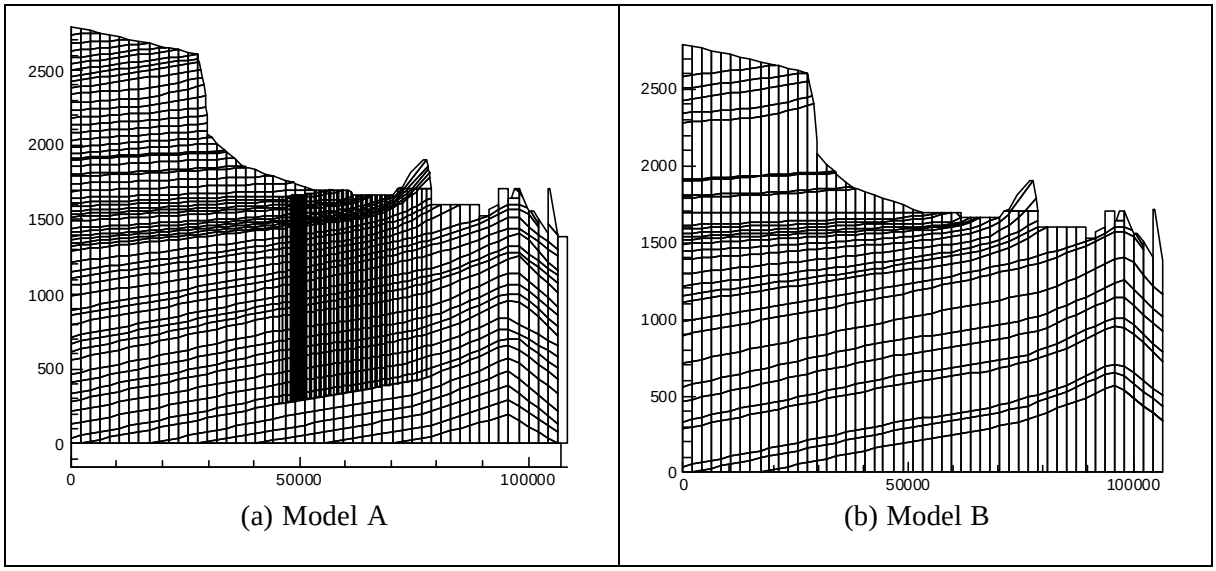

Figure 3: Mesh structure used for detailed flow calculations (a) and reactive chemical transport calculations (b)

Boundary Conditions

Boundary conditions for the numerical model are determined largely from the hydrological model discussed above and they can be summarized as

- Atmospheric pressure at the surface
- 20 cm precipitation on low (below 2000 masl) area with 2% infiltration
- 100 cm precipitation in the West decreasing to 20 cm at the base of the Wasatch Plateau with 15% infiltration
- Constant pressure on the Eastern boundary
- Constant pressure on Western boundary during sequestration simulations. No flow through this boundary during steady state calculations.
- No fluid flow through the base of the model
- Heat flow at the base of the model is set to match the typical terrestrial heat flow for the region.

Sequestration scenarios

Sequestration scenarios investigated fall into two groups. The first group used Model A and the TOUGH2 (Pruess 1991) simulator to model the injection of CO_2 into several reservoirs and tracked the location of the CO_2 over a period of 1000 years. Chemical reactions between the reservoir brine and the host rock were ignored. Reservoirs investigated were the Navajo Sandstone, White Rim Sandstone, Wingate Sandstone and Redwall Limestone aquifers.

The second group used the ChemTOUGH2 (White 1995) simulator and investigated the effects of water-rock interactions on CO_2 sequestration, firstly modeling reactions between a brine with a constant CO_2 partial pressure and reservoir rock and then a reactive transport simulation using Model B.

In all flow simulations reported CO_2 is injected for 30 years at 0.15 kg/s per meter of cross-section thickness. This rate corresponds to about 5 million tonnes / year (approximately equal to the emissions from a 600 MW coal fired power station) into a section 100 meters wide.

Model A Simulations

The Redwall Limestone proved unsuitable for long-term sequestration of CO_2 as very high injection pressures were required to inject into the medium permeability (2 mD) inferred for this reservoir. Figure 4 shows the fraction of injected CO_2 that has not returned to the atmosphere as a function of time. Clearly neither the Wingate nor Navajo formations appear suitable for long-term sequestration of CO_2. In both formations CO_2 begins to reach the surface before injection is completed. Even in the case of the White Rim Sandstone there is significant leakage from the target reservoir and a much larger volume of rock is exposed to CO_2 than just the White Rim sandstone formation (Figure 5).

Of the investigated reservoirs, only the White Rim formation may provide containment of injected CO_2 for the hundreds to thousands of years required for mineral sequestration reactions to complete. However, the geochemical situation is much more complex than has been assumed in Model A. Transport of reaction products in the reservoir, changing reservoir temperature, mineralogy and partial pressure of CO_2 all mean a full reactive transport model must be used.

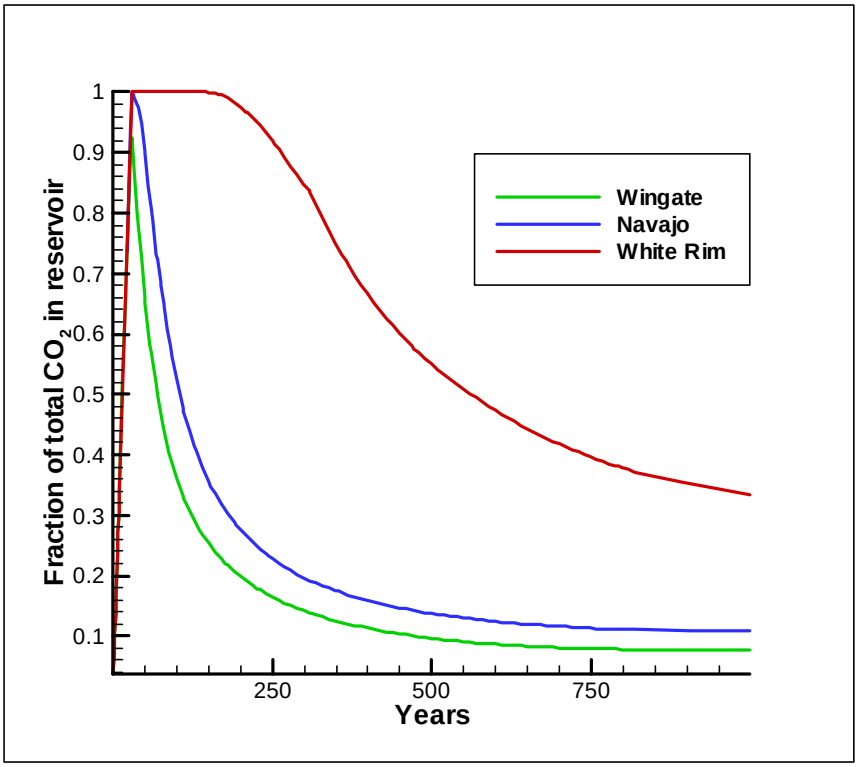

Figure 4: Fraction of total injected CO_2 remaining sub-surface as a function of time for three potential sequestration sites. Note that these calculations ignored water-rock reactions (i.e. Model A).

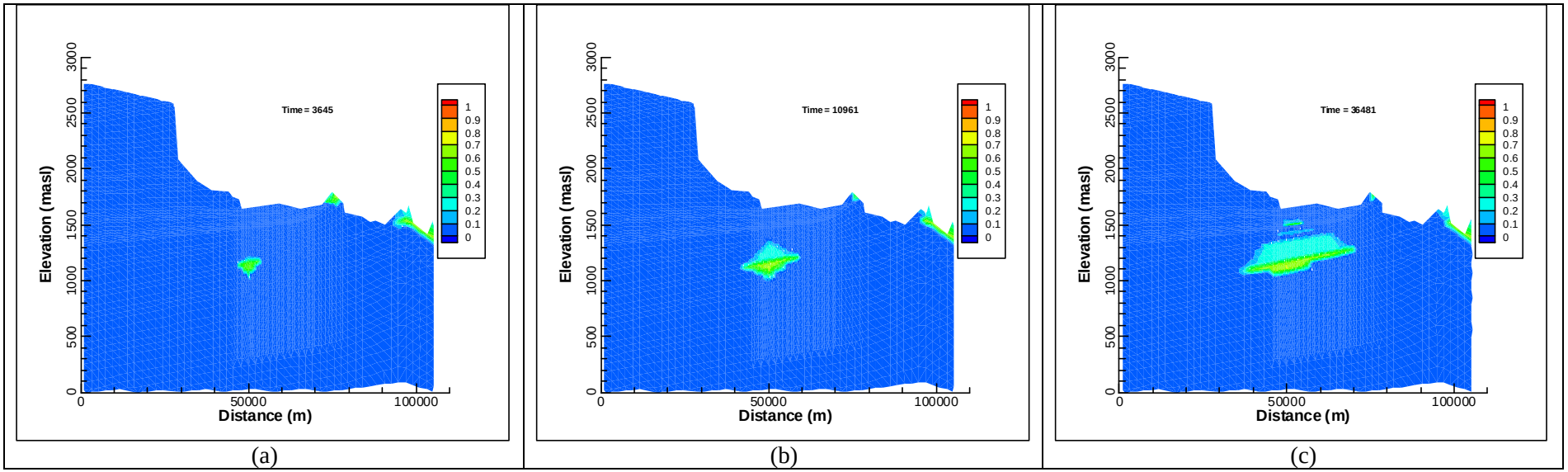

Figure 5: Gas saturation resulting from injection is into the White Rim formation at 10 (a), 30(b) and 100(c) years (Model A).

Model B Simulations

Reactive transport modeling is a computer intensive activity and a balance must be struck between model complexity, resolution and computer time. We have included sufficient geo-chemical complexity to represent the interaction of a simplified reservoir mineralogy (Table 2) with a CO_2 rich brine. To achieve this we used the lower spatial resolution of Model B (Figure 3). However it retains a reasonable resolution with over 1300 elements. The fate of injected CO_2 was traced for 1000 years as the geo-chemical calculations described earlier in this section suggest most sequestration reactions will be well advanced in this time. Details of parameters used for water-rock reaction rates and the kinetic model used for these reactions is provided in White *et al*. (2003).

Initial chemical conditions were calculated by firstly assigning the mineralogy specified in Table 2 to model elements, setting the reservoir fluid to a 0.3 M NaCl brine (based on water analyses from exploration wells in the San Rafael Swell region.) and then allowing the brine to react with the reservoir for 1000 years. This modified the original mineralogy slightly and provided initial conditions for the fluid reservoir throughout the reservoir. The initial brine composition in the White Rim sandstone is given in Table 3.

PH	Cl	SO4	HCO3	SiO_2	Al	Ca	Mg	K	Na	Fe	HS
11.7	10394	0.0	0.1	1442	0.0	3280	0.03	109	6709	0.0	0.1

Table 3: Initial water chemistry (in mg/kg) in White Rim sandstone reservoir

CO_2 was then injected into the White Rim formation for 30 years at the same rate as used in the non-reactive modeling (Model A). The chemistry and flows in the system were then simulated for a total of 1000 years.

The location of the gas at the conclusion of the simulation period is shown in Figure 6. Low permeability formations, primarily the Moenkopi and Chinle formations, have channeled the gas over thirty kilometers horizontally. There is some leakage into shallower permeable formations and the formation of secondary CO_2 reservoirs above the major concentration of gas in the White Rim and Black Box formations. Although it is not obvious from Figure 6, about 10% of the gas has escaped out the top boundary of the model.

Injected CO_2 dissolves in the reservoir brine to form a low pH fluid, this reacts with the feldspars in the reservoir and precipitates kaolinite together with the carbonate minerals calcite and dawsonite. These three secondary minerals have been observed as pore-filling minerals likely related to an influx of CO_2-rich fluids in the Springerville natural CO_2 field, eastern Arizona (Moore et al., 2003; these proceedings). Figures 7-9 show the change in the amount of feldspars throughout the model domain 950 years after injection begins. There is some dissolution of anorthite throughout the domain but it is largest in the area affected by the injected CO_2. K-feldspar is dissolved only in the low pH region formed by the interaction of injected CO_2 with the reservoir brine. Albite is initially supersaturated in some regions and there is some precipitation of albite where these regions are not affected by the injected CO_2. Albite is dissolved in the region affected by the injected CO_2. Figures 10-12 show the location of the precipitated minerals. These are largely confined to the two-phase, low pH region shown in Figure 6 although they are not found throughout this region. Calcite is not found shallower than 1500 masl while dawsonite and kaolinite are found deeper than 1600 masl. Dawsonite is not found in the Moenkopi or Chinle capping rocks.

Figure 13 shows the fate of the injected CO_2 950 years after injection began and these results are summarized in Table 4. It is not possible to directly compare the results of Model A (Figure 4) and Model B (Figure 13) as the coarse grid of Model B does introduce some errors into the calculation reducing the calculated leakage to the surface. In the long term, the effect of this discretization error is to overestimate the amount of CO_2 sequestered by about 10% .To make clear the effect of including water-rock reactions, also plotted in Figure 13 are the results of running the Model B grid using TOUGH2 rather that

ChemTOUGH2. The effect of including water-rock reactions is not simply to reduce the surface leakage by the amount of CO_2 sequestered in a mineral phase as precipitation of carbonate minerals also reduces the partial pressure of CO_2 reducing flows driven by pressure gradients. Although only 13% of the injected CO2 is sequestered as a mineral surface leakage is reduced by 60 %.

	With mineral sequestration	Without mineral sequestration
Gas phase	36 %	31 %
Dissolved in brine	34 %	31 %
Calcite	7 %	
Dawsonite mineral	6 %	
Leakage to surface	17 %	38 %

Table 4: Location of CO_2 950 years after the beginning of injection.

Summary and Conclusions

We have developed a conceptual and two numerical models of the geology and groundwater along a cross-section lying approximately NW-SE and in the vicinity of the Hunter power station on the Colorado Plateau, Central Utah. A number of potential sequestration sites were identified on this cross-section. However after initial modeling (ignoring water-rock interactions) of the fate of CO_2 injected into these sites only the White Rim Sandstone appeared to offer the properties that would make a successful sequestration site.

The capacity of White Rim sandstone for sequestration (assuming a 100 meter wide cross-section) is approximately $50{,}000 \times 100 \times 200 \times 22 = 2.2 \times 10^{10}$ kg or sufficient to sequester about 150 years of injected CO_2 (White *et al*. 2003). CO_2 is sequestered as a mineral or dissolved in reservoir fluid. In fact, a much larger volume of rock is 'seen' by the injected CO_2 than is contained in the White Rim formation (see Figure 7) and there should be ample volume of rock to sequester all the injected CO_2 providing flow to the surface is sufficiently slow.

More detailed modeling of injection into the White Rim Sandstone that included water-rock interactions was carried out. This found that 1000 years after the 30 year injection period began approximately 21 % of the injected CO_2 was permanently sequestered as a mineral, 52% was beneath the ground surface as a gas or dissolved in the groundwater and 17% had leaked to the surface. Leakage to the surface was continuing. Running model B ignoring water-rock interactions for a longer simulation period found gas ceased leaking to the surface at 1500 years. At this stage, by extrapolating Figure 14, we estimate at least 70% of the injected gas is permanently sequestered

A note of caution must be added to these estimates as some of the key parameters governing the results are not well known. In particular the composition and properties of the reservoir and seal units are not well known and nor are the mineral reaction rates or surface areas *in a field setting*.Better grid resolution is also required in the reactive transport model.

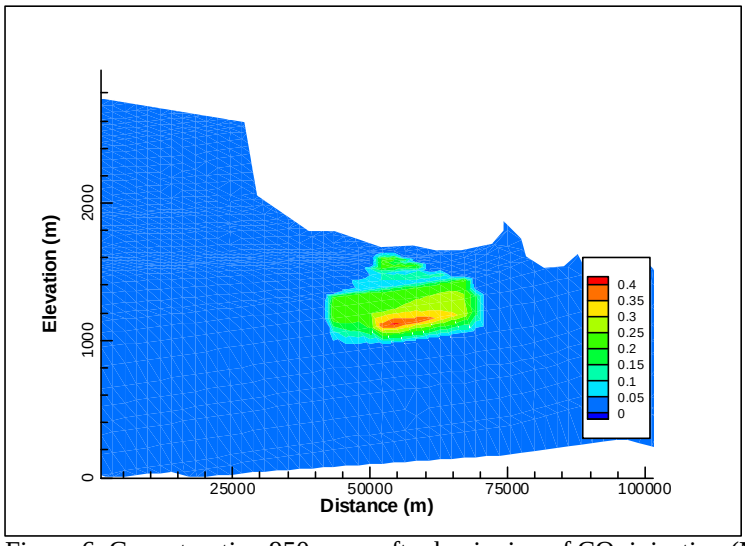

Figure 6: Gas saturation 950 years after beginning of CO_2 injection (Model B).

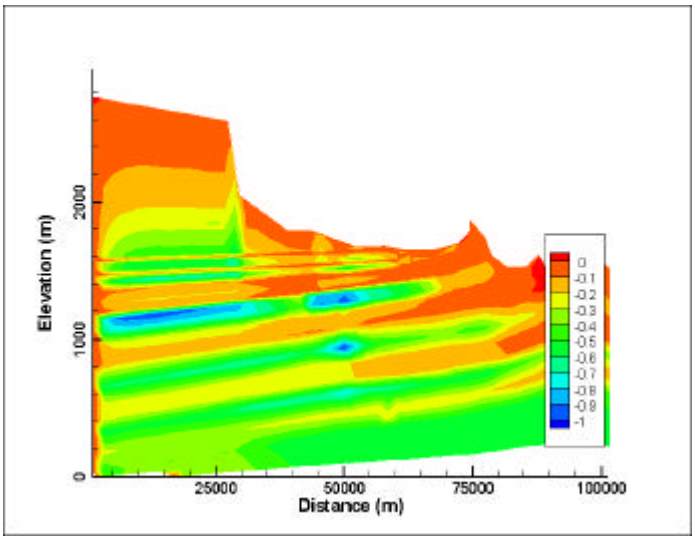

Figure 7: Change in anorthite density 950 years after the beginning of CO_2 injection (M dm^{-3}); (Model B).

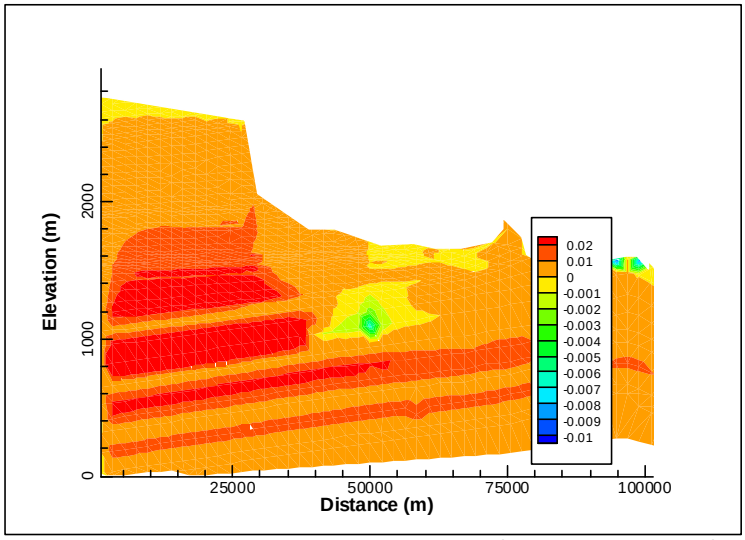

Figure 8: Change in albite density 950 years after the beginning of CO_2 injection (Mdm^{-3}Model B).

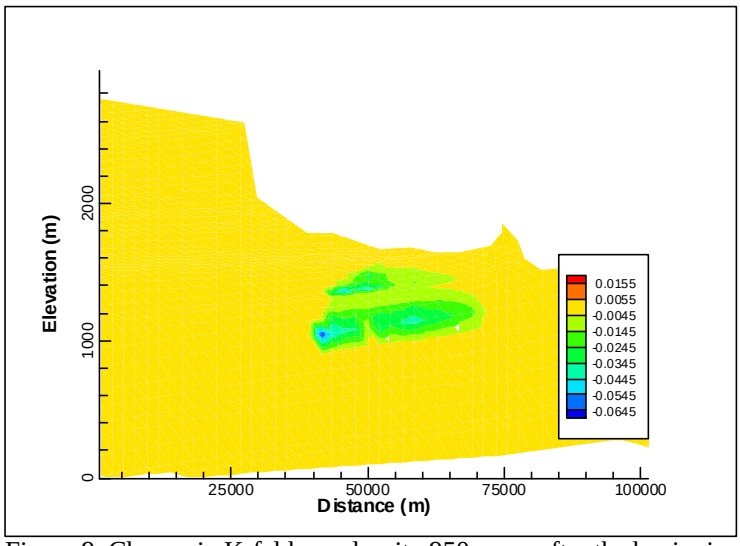

Figure 9: Change in K-feldspar density 950 years after the beginning of CO_2 injection (M dm^{-3}), (Model B).

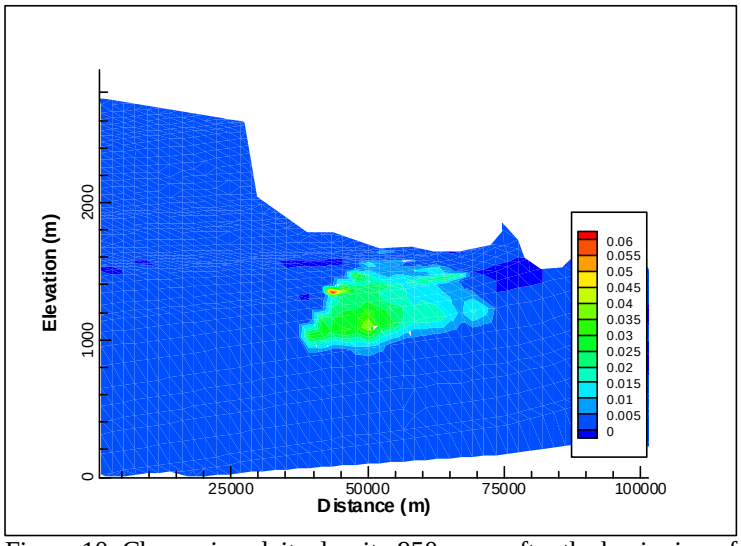

Figure 10: Change in calcite density 950 years after the beginning of CO2 injection (M dm^{-3}); (Model B).

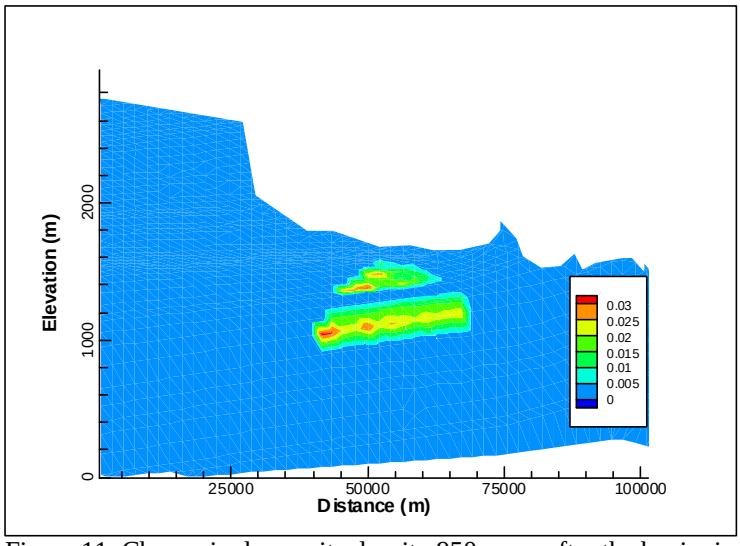

Figure 11: Change in dawsonite density 950 years after the beginning of CO_2 injection (M dm^{-3}; Model B).

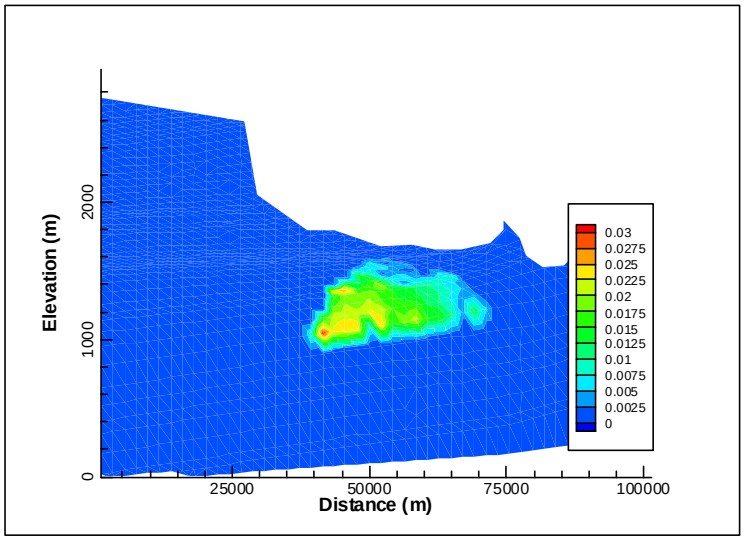

Figure 12: Change in kaolinite density 950 years after the beginning of CO_2 injection (M dm^{-3}; Model B).

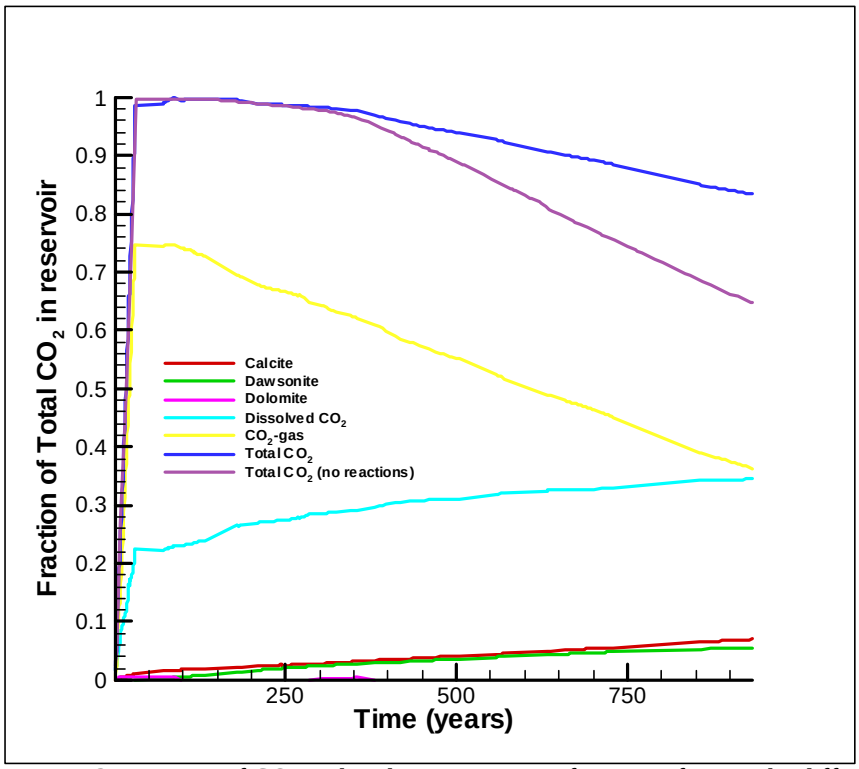

Figure 13: Location of CO_2 within the reservoir as a function of time. The difference between Total CO2 and 1.0 is the fraction of CO2 leakage to the atmosphere.

References

Allis, R., White, S., Chidsey, T., Gwynn, W., Morgan, C., Adams, M., Moore, J., 2001. Natural CO_2 Reservoirs on the Colorado Plateau and Southern Rocky Mountains: Candidates for CO_2 Sequestration, *Proceedings of the First National Conference on Carbon Sequestration*, Washington DC, May 2001.

Allis, R.G., Chidsey, T.C., Morgan. C, Moore, J. and White, S.P. 2003. CO_2 sequestration potential beneath large power plants in the Colorado Plateau-Southern Rocky Mountain region, USA. These Proceedings.

Danielson, T.W. and Hood, J.W., 1984. Infiltration to the Navaho sandstone in the Lower Dirty Devil River Basin, Utah, with emphasis on techniques used in its determination. *U.S. Geol. Surv. Water Investigations Report 84-4154*, p. 45.

Freethey, G.W. and Cordy, G. 1991. Geohydrology of Mesozoic rocks in the Upper Colorado River Basin in Arizona, Colorado, New Mexico, Utah, and Wyoming, excluding the San Juan Basin. *U.S. Geol. Surv. Prof. Paper 11411-C*, p. 118.

Moore J., Adams, M., Allis, R.G., Lutz, S., Rauzi, S. 2003. CO_2 mobility in natural reservoirs beneath the Colorado Plateau – Southern Rocky Mountains: an example from Springerville – St. Johns field, Arizona, New Mexico. These Proceedings, and submitted to Chemical Geology, special issue on Geological CO_2 sequestration.

Perkins, E.H. and Gunter, W.D., 1995. Aquifer disposal of CO2-rich greenhouse gases: Modelling of water-rock reaction paths in a siliciclastic aquifer. In Water-rock Interactions (Y.K. Kharaka and O.V. Chudaev (editors)), pp895-898 Rotterdam, Brookfield.

Pruess, K., 1991. TOUGH2 - *A general purpose numerical simulator for multiphase fluid and heat flow* Rep LBL-29400, Lawrence Berkeley Lab., Berkeley, Calif.

Rush, F.E., Whitfield, M.S. and Hart, I.M. 1982. Regional hydrology of the Green River-Moab area, Northwestern Paradox basin, Utah. *U.S. Geol Surv. Open-File Report 82-107*, p. 86, Denver, CO.

White, S., Weir, G. and Kissling, W., 2001. Numerical Simulation of CO_2 Sequestration in Natural CO_2 Reservoirs on the Colorado Plateau, *Proceedings of the First National Conference on Carbon Sequestration*, Washington DC, May 2001.

White, S., Allis, R., Moore , J., Chidsey, T., Morgan, C., Gwynn, W.and Adams, M., 2002. Natural CO_2 Reservoirs on the Colorado Plateau and Southern Rocky Mountains, USA, A Numerical Model. *Proc. Greenhouse Gas Control Technologies 6th Conference*, Kyoto, Japan Oct. 2002

White, S., Allis, R., Moore , J., Chidsey, T., Morgan, C., Gwynn, W.and Adams, M., 2003.Simulation of reactive transport of injected CO_2 on the Colorado Plateau, Utah, USA. Submitted to Chemical Geology special issue on Geological CO_2 sequestration.

White, S.P., 1995. Multiphase non-isothermal transport of systems of reacting chemicals. Water Resources Res. 31(7), 1761-1772.

Table 2:
Initial Reservoir Mineralogy (Volume %). The code for formation names is given in Table 1.

Formation	Anorthite	Na-Smectite	Calcite	Dolomite	K-Feldspar	Kaolinite	Quartz	Gypsum	Illite	Hematite	Magnetite	Albite	Dawsonite	Siderite	Porosity
Tkn		34.	1.	1.		34.	18.		1.						10.
Tkn	1.	11.	2.		1.	11.	63.		1.			1.			10.
Kpr	1.	11.	2.		1.	11.	63.		1.	0.	0.	1.		0.	10.
Kc	1.	11.	2.		1.	11.	67.		1.	0.	0.	1.	0.	0.	5.
Kbh	1.	11.	2.		1.	11.	63.		1.	0.	0.	1.	0.	0.	10.
Ksp	1.	11.	2.		1.	11.	67.		1.	0.	0.	1.	0.	0.	5.
Kmm		37.	1.	1.		37.	20.		1.	0.	0.	0.	0.	0.	2.
Kmeu	1.	12.	2.		1.	12.	69.		1.	0.	0.	1.	0.	0.	2.
Kmem	0.	6.	1.			6.	35.		0.	0.	0.	0.	0.	0.	5.
Kmel	0.	4.	1.			4.	23.		0.	0.	0.	0.	0.	0.	2.
Kmbg	1.	12.	2.		1.	12.	69.		1.	0.	0.	1.	0.	0.	2.
Kmf		15.	2.	1.		15.	61.		1.	1.	1.	0.	0.	0.	2.
Kdc		29.	1.	1.		29.	29.		1.	0.	0.	0.	0.	0.	10.
Jmbb	1.	11.	2.	1.	1.	11.	68.		0.	1.	1.	1.	0.	0.	2.
Jms		13.	2.	1.		13.	65.		1.	1.	1.	0.	0.	0.	2.
Js	1.	11.	2.	1.	1.	11.	68.	1.	0.	0.	0.	1.	0.	0.	2.
Je	1.	5.	1.	1.	1.	5.	75.		0.	1.	1.	1.	0.	0.	10.
Jc	1.	10.	1.	52.	1.	10.	21.		1.	0.	0.	1.	0.	0.	2.
Jn	1.	2.	1.	1.	1.	2.	73.		0.	1.	1.	1.	0.	0.	20.
Jk	1.	8.	1.		1.	8.	65.		0.	0.	0.	1.	0.	0.	20.
Jw	1.	8.	1.		1.	8.	65.		0.	0.	0.	1.	0.	0.	20.
Trc	1.	22.	2.	2.	1.	22.	44.		1.	1.	1.	1.	0.	0.	2.
Trm	1.	22.	2.	5.	1.	22.	43.		0.	2.	0.	1.	0.	0.	2.
Pk		2.	2.	65.		2.	19.		0.	0.	0.	0.	0.	0.	10.
Pwr	1.	2.	2.		1.	2.	75.		0.	0.	0.	1.	0.	0.	20.
Pec				59.			39.		0.	0.	0.	0.	0.	0.	2.
Pht				28.		16.	47.		0.	2.	0.	0.	0.	0.	10.
Pp		9.		27.		9.	45.		0.	0.	0.	0.	0.	0.	10.
Ppt		37.	1.	1.		37.	20.		1.	0.	0.	0.	0.	0.	2.
Mr				90.					0.	0.	0.	0.	0.	0.	10.
Do				98.					0.	0.	0.	0.	0.	0.	2.
De		20.		59.		20.			0.	0.	0.	0.	0.	0.	2.
Clm		20.		59.		20.			0.	0.	0.	0.	0.	0.	2.
Co		20.		59.		20.			0.	0.	0.	0.	0.	0.	2.
Ct							98.		0.	0.	0.	0.	0.	0.	2.